JOURNAL OF Materials CHEMISTRY

Synthesis and characterization of a pipe-structure manganese vanadium oxide by hydrothermal reaction

Fan Zhang, Peter Y. Zavalij and M. Stanley Whittingham*

Materials Research Center and Chemistry Department, State University of New York at Binghamton, Binghamton, NY 13902-6000, USA. E-mail: stanwhit@binghamton.edu

Received 28th May 1999, Accepted 14th September 1999

A novel manganese vanadium oxide has been synthesized using the hydrothermal reaction of vanadium(v) pentoxide with manganese(II) sulfate with an organic templating cation at 165 °C. The $(Mn^{2+})_6(Mn^{3+})_{1-2/3z}$-$(OH)_3(VO_4)_3[(VO_4)_{1-2z}(V_2O_7)_z]$ ($z=0.2$) phase has a hexagonal tunnel structure and space group $P6_3mc$. The cell parameters of this compound are $a=13.229(1)$ and $c=5.255(1)$ Å. This compound was also characterized by electron microprobe analysis, FTIR, TGA as well as electrochemically and reacted readily with lithium in electrochemical cells.

Introduction

Soft chemistry has been shown to be an effective method for the preparation of transition metal oxides that offer many advantages as cathodes in rechargeable lithium batteries. There has been much interest in the last two decades in layered or opened vanadium oxides and their intercalates because of their potential use as secondary cathode materials for advanced lithium batteries. Therefore, the already rich crystal chemistry of the vanadates with open frameworks was considerable replenished with many new structures. A significant part of them were done in our group. Earlier we reported the use of the tetramethylammonium ion as a structure-directing cation[1] and showed that a number of new phases of tungsten,[2,3] molybdenum[4,5] and vanadium could be formed.[6] For vanadium, two new structure types were reported in 1995,[6] the layered $NMe_4V_4O_{10}$[7] and a hydrated vanadium dioxide.[8,9] Subsequently, several other layer structure vanadium oxides containing organic species were formed.[10–14] A double vanadium oxide sheet structure was formed by iron chloride and vanadium oxide, the layered $[NMe_4]_zFe_y$-$V_2O_5{\cdot}nH_2O$, where z is 1/6, $y\approx0.1$ and n is 1/ 6.[15] To date the tetramethylammonium ion has shown the ability to form the widest range of different structures with differing organic to vanadium ratios;[16] the present count is six structures including two with a string-like morphology formed at pH values of 3 or less, $NMe_4V_3O_7$[17] and $[NMe_4]_5V_{18}O_{45}$.[18] Recently, four new zinc vanadium compounds, $Zn_{0.4}V_2O_5{\cdot}0.27H_2O$, $[NMe_4]_{0.5}Zn_{0.39}V_2O_5$, $Zn_3(OH)_2(V_2O_7){\cdot}H_2O$ and $Zn_2(OH)_3$-(VO_3), with layered structures were reported.[19,20]

Lithium batteries are presently used in a range of consumer applications, such as cellular phones and portable computers. These use lithium carbon-based anodes, and predominantly $LiCoO_2$ as the cathode. However, cobalt is too expensive for large applications and there is an active search for replacement transition metal oxides. Such oxides should readily intercalate lithium ions in a reversible manner. Manganese and vanadium oxides are particularly attractive because they tend to form structures that can incorporate ions such as lithium. However, Li_xMnO_2, which has a similar layered structure to Li_xTiS_2 and Li_xCoO_2, tends to convert to the spinel form $LiMn_2O_4$ on cycling the lithium.[21] One way to stabilize the layered MnO_2 lattice is to place pillaring ions, such as potassium or vanadium oxide species between the layers.

This work reports the synthesis and structural characterization of the novel compound $(Mn^{2+})_6(Mn^{3+})_{1-2/3z}(OH)_3$-$(VO_4)_3[(VO_4)_{1-2z}(V_2O_7)_z]$ ($z=0.2$). It was prepared by reaction of V_2O_5 with $MnSO_4$ in water in the presence of an organic cation, tetraethylammonium hydroxide, respectively. The tendency of tetraalkylammonium cations to direct the synthesis toward opened structures has been previously noted.[1,6]

Experimental

The manganese vanadium oxide compound was prepared by hydrothermal treatment of V_2O_5 and $MnSO_4$ or $Mn(MeCO_2)_2$ powder (Johnson) and tetraethylammonium hydroxide solution (Aldrich) in a 1 : 1 : 4 molar ratio, respectively; the pH of this solution was 10.20. The reaction mixture was heated in a 125 ml Teflon-lined Parr Bomb reactor for 72 h at 165 °C. The resulting large dark brown pipe crystals were filtered off and dried in air. The pH (9.82) of the solution after reaction was basic. At lower organic concentrations, for example for $Mn(CH_3CO_2)_2 : V_2O_5 : NEt_4OH$ reactant ratios of 1 : 1 : 1 and 1 : 1 : 3, MnV_2O_6 and $Mn_2V_2O_7$ are formed, respectively.

X-Ray powder diffraction was performed using Cu-Kα radiation on a Scintag diffractometer equipped with a solid state detector. The powder sample was homogenized using 30 μm sieves.

TGA data were obtained on a Perkin-Elmer model TGA 7, FTIR on a Perkin-Elmer 1500 series, and SEM images on a JEOL8900 electron microprobe.

Initial electrochemical studies were conducted in lithium cells using 1.5 M $LiPF_6$ in dimethyl carbonate–ethylcarbonate (2 : 1) as electrolyte. The vanadium oxide was mixed with 10% carbon black and 10% Teflon powder, and hot pressed for 20 min at 167 °C. A MacPile potentiostat was used to cycle the cells.

Results and discussion

The morphology of the manganese compound was well-formed dark brown large hexagonal channels, as shown in Fig. 1. Electron microprobe analysis showed that they contained manganese and vanadium but no sulfur and suggested a *ca.* 1 : 1 ratio of manganese to vanadium. The pH of the reaction medium remained alkaline, starting at 10.2 and finishing at 9.8 suggesting that the vanadium will be present as VO_4 tetrahedra.[16]

TGA analyses of the manganese compound run at 1 °C min^{-1} in oxygen and nitrogen are shown in Fig. 2. The small weight losses suggest that no organic matter is present; moreover, organic material typically is lost in a rather sharp

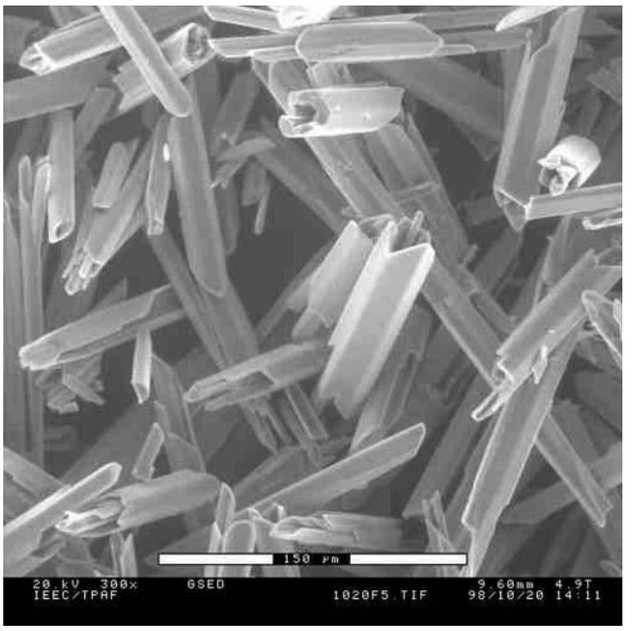

Fig. 1 SEM image of manganese vanadium oxide.

transition.[16] The small weight loss of *ca.* 2 and 4% (under O_2 and N_2, respectively) over the wide temperature range suggests the presence of hydroxy groups; these are lost as water leading to the lower weight loss in oxygen where re-oxidation of the oxide can be seen at *ca.* 400 °C. The expected weight losses are 1.2 and 3.1% respectively; the larger observed values are probably due to loss of some surface species and slight chemical reduction of the manganese at higher temperatures. X-Ray diffraction shows no obvious structural change up to 400 °C apart from a lattice contraction; however, by 550 °C in oxygen, the product is a mixture of $Mn_2V_2O_7$ and Mn_2O_3.

The FTIR spectrum has no sharp absorption peaks but a broad absorption from 600 to 1000 cm^{-1} typical of pyrovanadates and other tetrahedral vanadates. The paucity of V–O bands mitigates against the presence of vanadium clusters. Broad absorption above 1200 cm^{-1} precludes the observation of OH bands.

The X-ray diffraction pattern of the manganese compound (Fig. 3), can be indexed in the hexagonal lattice system with space group $P6_3mc$ using the TREOR program.[22] The cell parameters of this compound are $a=13.229(1)$ and $c=5.2547(1)$ Å. The crystal structure was solved by direct methods and refined using CSD software.[23] The final Rietveld refinement was done with GSAS software.[24] The experimental, calculated and difference plots are shown in Fig. 3. All experimental and crystallographic data are given in Table 1 while atomic coordinates, displacement parameters and occupation factors are listed in Table 2. The title structure appeared not to be completely ordered and occupation factors of Mn2, V2a, V2b and O6 were refined first as independent parameters and then after their sense was figured out, the restraints described in Table 2 were employed.

Both types of manganese atoms (divalent Mn1 and trivalent Mn2) have octahedral coordination. The framework of the title structure consists of a 3D skeleton of face- and edge-sharing Mn^{2+} octahedra. Two of them share faces and the resulting pairs join along the *z*-axis by sharing edges and form double chains which in their turn share corners giving a 3D net with hexagonal and trigonal tunnels (Fig. 4). The walls of the hexagonal tunnel (0,0,*z*) are lined with tetrahedral vanadate (V1) ions VO_4^{3-} giving a smaller tunnel which is in turn filled with Mn^{3+} octahedra. The average Mn–O distance for this type of octahedron is 2.25 Å *cf.* 2.15 Å for the Mn^{2+} octahedra (Table 3). The trigonal tunnels (1/3,2/3,*z*) consist of continuous chains of oxygen tetrahedra which alternate in sharing corners (O6 atom) and faces (three O4 atoms). In the ideal case every other tetrahedron is occupied by a vanadium atom, and the trigonal tunnel is filled with VO_4^{3-} as shown in Fig. 5(a). This gives the ideal formula $Mn^{II}_6Mn^{III}(OH)_3(VO_4)_4$.

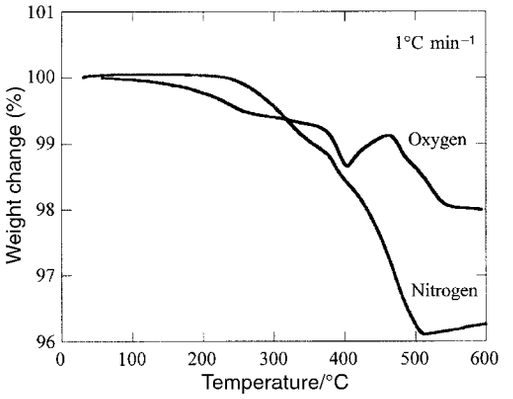

Fig. 2 TGA pattern of manganese vanadium oxide.

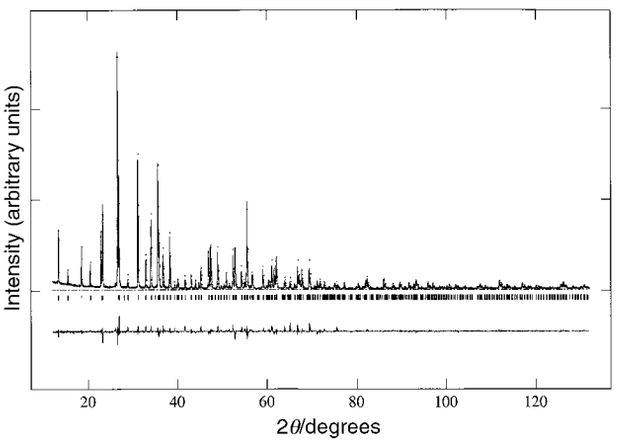

Fig. 3 Experimental (solid line), calculated (small circles) and difference (bottom) plot for $Mn_{7-2/3z}(OH)_3(VO_4)_{4-2z}(V_2O_7)_z$. Vertical lines show reflection positions (Cu-Kα_1 and Cu-Kα_2 radiation).

Table 1 Crystallographic data for $Mn_{7-2/3z}(OH)_3(VO_4)_{4-2z}(V_2O_7)_z$

	$Mn_{7-2/3z}(OH)_3(VO_4)_{4-2z}$-$(V_2O_7)_z$, $z=0.199(3)$
Compound	
Space group	$P6_3mc$
a/Å	13.2293(1)
c/Å	5.25472(6)
Cell volume/$Å^{-3}$	796.44(2)
D_c/g cm^{-3}	3.711
M	890.1
μ/cm^{-1}	6.722
Radiation (λ/Å)	Cu-Kα (1.54178)
Diffractometer	Scintag XDS2000
Scan range, 2θ/°	12–132
Step, 2θ/°	0.01
Exposure/s $point^{-1}$	30
Indexing method	TREOR[23]
Structure determination	Direct methods
Software	CSD[24]
Final refinement	GSAS[25]
Mode of refinement	Full profile
Number of refined parameters	37
Number of reflections	301
Preferred orientation, Marsh–Dollase	$R_0=1.244$ along 100 axis
$R(F^2)$	0.087
$R(p)$	0.085
$Rw(p)$	0.112
Max. Δ/σ	0.01

Table 2 Atomic parameters for $Mn_{7-2/3z}(OH)_3(VO_4)_{4-2z}(V_2O_7)_z$

Atom	*x/a*	*y/b*	*z/c*	$10^2\ U_{iso}/Å^2$	Wyckoff position	Occupancy (*g*)[a]
Mn1	0.42632(8)	0.07902(7)	−0.0137(6)	1.24(4)	12d	1
Mn2	0	0	0.8046(8)	1.24(4)	2a	0.868(2)
V1	0.15073(6)	−0.15073(6)	0.0112(7)	1.01(5)	6c	1
V2a	1/3	2/3	0.7516(8)	1.01(5)	2b	0.801(3)
V2b	1/3	2/3	0.464(4)	1.01(5)	2b	0.199(3)
O1	0.0726(3)	0.3397(3)	0.8404(8)	0.46(7)	12d	1
O2	0.8123(2)	−0.8123(2)	0.7917(12)	0.46(7)	6c	1
O3	0.5262(2)	−0.5262(2)	0.6991(13)	0.46(7)	6c	1
O4	0.4002(2)	−0.4002(2)	0.6279(13)	0.46(7)	6c	1
O5	0.9199(2)	−0.9199(2)	0.5583(15)	0.46(7)	6c	1
O6	1/3	2/3	0.125(3)	0.46(7)	2b	0.801(3)

*$g_{V2a} = g_{O6} = 1 - g_{V2b}$; $g_{Mn2} = 1 - 2/3 g_{V2b}$.

Table 3 Bond lengths (Å) for $Mn_{7-2/3z}(OH)_3(VO_4)_{4-2z}(V_2O_7)_z$

Mn1–O1	2.196(3)	V1–O1	1.629(4) (×2)
Mn1–O1′	2.164(4)	V1–O2	1.700(6)
Mn1–O2	2.130(4)	V1–O5	1.638(4)
Mn1–O3	2.148(6)	V2a–O4	1.664(5) (×3)
Mn1–O3′	2.400(5)	V2a–O6	1.963(14)
Mn1–O4	2.169(4)	V2b–O4	1.757(12) (×3)
Mn2–O5	2.245(6) (×3)	V2b–O6	1.781(25)
Mn2–O5′	2.268(6) (×3)		

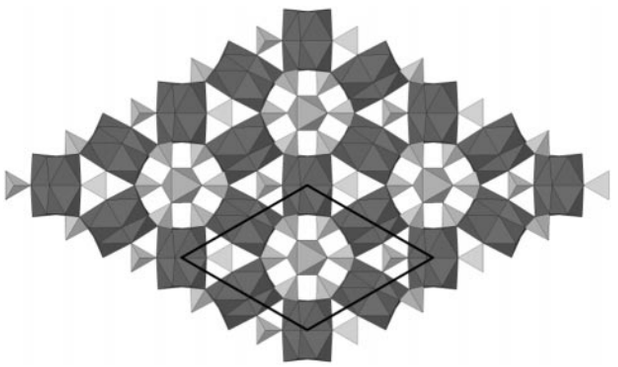

Fig. 4 Crystal structure of $Mn_{7-2/3z}(OH)_3(VO_4)_{4-2z}(V_2O_7)_z$ in projection along the *z*-axis. Mn^{2+} octahedra are dark gray and Mn^{3+} are light gray.

However, the structure deviated from ideality. In the trigonal tunnels, the distribution of the V atoms is somewhat disordered, so that some tetrahedra point up the tunnels and some down. One orientation is 80% occupied with V1a atoms whereas the other is 20% occupied with V1b atoms. Two possible distributions of these oppositely directed VO_4 tetrahedra are shown in Fig. 5. The change in orientation can occur at a V_2O_7 group as shown in Fig. 5(b), where opposite tetrahedra form a pair through an apical oxygen (O6), or at a vanadium vacancy, as shown in Fig. 5(c). A third model, where two VO_4 tetrahedra share a base, was not considered because the V–O–V distance would be too short. For both the fully

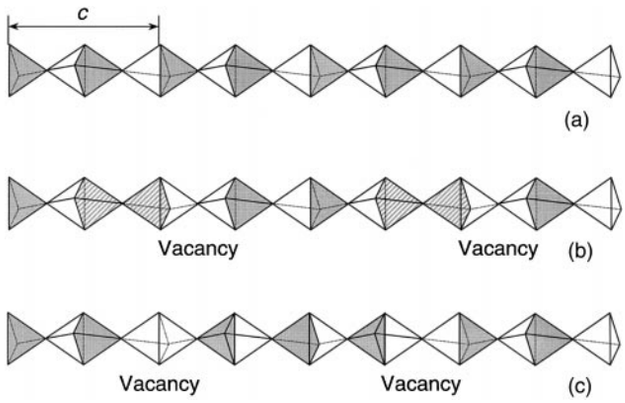

Fig. 5 Possible distribution of VO_4 tetrahedra in trigonal tunnels: (a) ordered VO_4, (b) disordered VO_4 and V_2O_7, and (c) disordered VO_4.

ordered structure [Fig. 5(a)] and the disordered V_2O_7 model [Fig. 5(b)] one half of the tetragonal cavities are occupied by vanadium atoms and the other half are empty. However, for the vanadium vacancy model [Fig. 5(c)] more cavities are empty than occupied and this difference is equal to the number of faults in packing VO_4 groups along the trigonal tunnel. In both of these models there are vacancies of the shared oxygen (O6) along the tunnel. In Fig. 5(b) there are two types of vanadate groups present: orthovanadate VO_4^{3-} and pyrovanadate $V_2O_7^{4-}$, and their refined occupancies are 60 and 20%, respectively. Thus 20% of the corner-shared O6 are absent. The charge imbalance caused by these vacancies can be compensated either by some manganese vacancies, or by hydrogen loss from some of the OH groups. Rietveld refinement confirmed partial occupancy for the O6 and trivalent Mn2 sites. Therefore the final compositions for the title compound is $Mn^{II}_6Mn^{III}_{1-2/3z}(OH)_3(VO_4)_{4-2z}(V_2O_7)_z$, where $z = 0.199(3)$. The value of *z* probably depends on how the compound is prepared and may vary within the range 0–0.5 giving the compositions $Mn_7(OH)_3(VO_4)_4$ and $Mn_{7-1/3}(OH)_3(VO_4)_3(V_2O_7)_{1/2}$, respectively for the end members. These two extreme representatives have structures with trigonal tunnels filled with orthovanadate or pyrovanadate ions only.

There are two groups of other structures with the same 3D-

Table 4 Comparison of $Mn_{7-2/3z}(OH)_3(VO_4)_{4-2z}(V_2O_7)_z$ with related structures

Site	$Mn_{7-2/3z}(OH)_3(VO_4)_{4-2z}(V_2O_7)_z$	$Zn_7(OH)_3(VO_4)_3(SO_4)$[a]	$M_{5.5}(OH)_3(HPO_3)_4$[b]	$Co_{5.5}(OH)_3(HPO_3)_4$[c]
12d	Mn^{2+}	Zn^{2+}	≈11/12 M^{2+}	≈11/12 Co^{2+}
2a	$(1-2/3z)\ Mn^{3+}$	Zn^{2+}	—	—
6c	OH^-	OH^-	OH^-	OH^-
6c′	VO_4^{3-}	VO_4^{3-}	HPO_3^{2-}	HPO_3^{2-}
2b	$(1-2z)\ VO_4^{3-}$, $z1/2\ V_2O_7^{4-}$	SO_4^{2-}	HPO_3^{2-}	$(1-x)\ HPO_3^{2-}$
2b′	$z\ 1/2\ V_2O_7^{4-}$	—	—	$x\ HPO_3^{2-}$

[a]Ref. 24. [b]M = Mn, Fe (ref. 25); M = Zn (ref. 27); M = Ni (ref. 26). [c]Ref. 26.

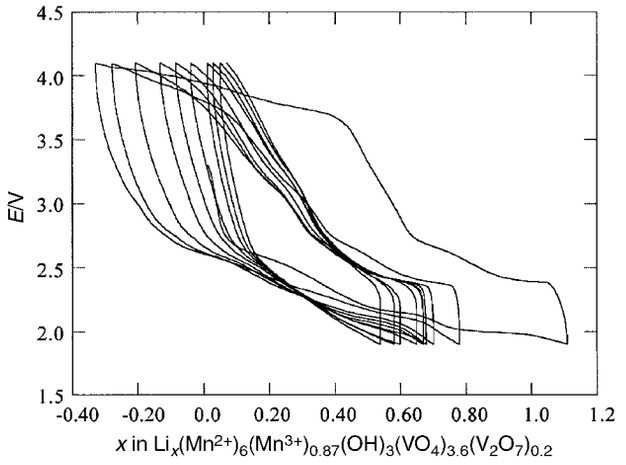

Fig. 6 Electrochemical cycling of manganese vanadium oxide.

skeleton but with different distributions and compositions of tetrahedra and octahedra in the hexagonal and trigonal tunnels. The first,[25] $Zn_7(OH)_3(VO_4)_3(SO_4)$ can be derived from ideal $Mn_{7-2/3z}(OH)_3(VO_4)_{4-2z}(V_2O_7)_z$ structure as follows: $z=0$, Mn^{2+} is substituted by Zn^{2+}, the Mn^{3+} positions are fully occupied by divalent Zn^{2+} and the trigonal tunnels are filled with SO_4^{2-} instead of VO_4^{3-} to give charge balance with no disorder. The second type is $M^{2+}{}_{6-z}(OH)_3(HPO_3)_4$ (M = Mn, Fe,[26] Co, Ni,[27] Zn[28]) where all tetrahedra are HPO_3^{2-} groups and the Mn^{3+} positions in the middle of hexagonal tunnels are unoccupied owing to the orientation of HPO_3^{2-} ions with H atoms directed inside the tunnel. The distribution of these different ions are compared in Table 4.

The electrochemical behavior of the $(Mn^{2+})_6(Mn^{3+})_{1-2/3z}(OH)_3(VO_4)_3[(VO_4)_{1-2z}(V_2O_7)_z]$ ($z=0.2$) phase is shown in Fig. 6. When there is no lithium present in the compound, it has an initial cell voltage of 3.3. Only 1.15 lithium per formula unit could be incorporated into the structure on discharge above 2 V, consistent with the difficulty of reducing tetrahedral vanadium.[29] The divalent manganese will probably not be reduced at potentials above 2 V relative to lithium.

Conclusions

A new hexagonal manganese vanadium oxide, $(Mn^{2+})_6(Mn^{3+})_{1-2/3z}(OH)_3(VO_4)_3[(VO_4)_{1-2z}(V_2O_7)_z]$ ($z=0.2$), with a hexagonal tunnel morphology has been synthesized hydrothermally and structurally characterized. Mild hydrothermal reactions appear to be a generally useful method for the synthesis of transition metal oxides. In many cases, new structures are formed as recently observed for tungsten, molybdenum and vanadium. Extensive research is now underway to explore the possibilities of this approach in the preparation of new materials, and has recently been reviewed.[16,30]

Acknowledgements

We thank the National Science Foundation through grant DMR-9810198 for partial support of this work. We also thank Bill Blackburn for the electron microprobe studies.

References

1 M. S. Whittingham, J. Li, J. Guo and P. Zavalij, *Mater. Sci. Forum*, 1994, **152–153**, 99.
2 K. P. Reis, A. Ramanan and M. S. Whittingham, *Chem. Mater.*, 1990, **2**, 219.
3 K. P. Reis, A. Ramanan and M. S. Whittingham, *J. Solid State Chem.*, 1992, **96**, 31.
4 J. Guo, P. Zavalij and M. S. Whittingham, *Chem. Mater.*, 1994, **6**, 357.
5 J. Guo, P. Zavalij and M. S. Whittingham, *Eur. J. Solid State Chem.*, 1994, **31**, 833.
6 M. S. Whittingham, J. Guo, R. Chen, T. Chirayil, G. Janauer and P. Zavalij, *Solid State Ionics*, 1995, **75**, 257.
7 P. Zavalij, M. S. Whittingham, E. A. Boylan, V. K. Pecharsky and R. A. Jacobson, *Z. Kristallogr.*, 1996, **211**, 464.
8 T. Chirayil, P. Zavalij and M. S. Whittingham, *Solid State Ionics*, 1996, **84**, 163.
9 T. Chirayil, P. Zavalij and M. S. Whittingham, *J. Electrochem. Soc.*, 1996, **143**, L193.
10 D. Riou and G. Férey, *J. Solid State Chem.*, 1995, **120**, 137.
11 D. Riou and G. Férey, *Inorg. Chem.*, 1995, **34**, 6520.
12 D. Riou and G. Férey, *J. Solid State Chem.*, 1996, **124**, 151.
13 L. F. Nazar, B. E. Koene and J. F. Britten, *Chem. Mater.*, 1996, **8**, 327.
14 Y. Zhang, J. R. D. DeBord, C. J. O'Connor, R. C. Haushalter, A. Clearfield and J. Zubieta, *Angew. Chem., Int. Ed. Engl.*, 1996, **35**, 989.
15 F. Zhang, P. Y. Zavalij and M. S. Whittingham, *Mater. Res. Bull.*, 1997, **32**, 701.
16 T. A. Chirayil, P. Y. Zavalij and M. S. Whittingham, *Chem. Mater.*, 1998, **10**, 2629.
17 T. A. Chirayil, P. Y. Zavalij and M. S. Whittingham, *Chem. Commun.*, 1997, 33.
18 B. E. Koene, N. J. Taylor and L. F. Nazar, *Angew. Chem.*, 1999, in press.
19 F. Zhang, P. Y. Zavalij and M. S. Whittingham, *Mater. Res. Soc. Symp. Proc.*, 1998, **496**, 367.
20 P. Y. Zavalij, F. Zhang and M. S. Whittingham, *Acta Crystallogr., Sect. C*, 1997, **53**, 1738.
21 R. Chen and M. S. Whittingham, *J. Electrochem. Soc.*, 1997, **144**, L64.
22 P.-E. Werner, L. Eriksson and M. Westdahl, *J. Appl. Crystallogr.*, 1985, **18**, 367.
23 L. G. Akselrud, P. Y. Zavalii, Y. N. Grin, V. K. Pecharsky, B. Baumgartner and E. Wolfel, *Mater. Sci. Forum*, 1993, **133–136**, 335.
24 A. C. Larson and R. B. VonDreele, GSAS, General Structure Analysis System, User Guide, Los Alamos National Laboratory, Los Alamos, NM, USA, 1994.
25 K. Kato, Y. Kanke, Y. Oka and T. Zao, *Z. Kristallogr.*, 1998, **213**, 26.
26 M. P. Attfield, R. E. Morris and A. K. Cheetham, *Acta Crystallogr., Sect. C*, 1994, **50**, 981.
27 M. D. Marcos, P. Amoros, A. Beltran-Porter, R. Martinez-Manez and J. P. Attfield, *Chem. Mater.*, 1993, **5**, 121.
28 M. D. Marcos, P. Amoros and A. Le-Bail, *J. Solid State Chem.*, 1993, **107**, 250.
29 P. Y. Zavalij and M. S. Whittingham, *Acta Crystallogr., Sect. B*, 1999, **55**, 627.
30 M. S. Whittingham, *Curr. Opin. Solid State Mater. Sci.*, 1996, **1**, 227.

Paper 9/07465A